Estrogen receptor α (ERα)-binding super-enhancers drive key mediators that control uterine estrogen responses in mice

Sylvia C. Hewitt[1],* **Sara A. Grimm**[2], **San-Pin Wu**[1], **Francesco J. DeMayo**[1], and **Kenneth S. Korach**[1]

From the [1]*Reproductive and Developmental Biology Laboratory and the* [2]*Integrative Bioinformatics Support Group, NIEHS, National Institutes of Health, Research Triangle Park, North Carolina, USA*

Edited by John M. Denu

Estrogen receptor α (ERα) modulates gene expression by interacting with chromatin regions that are frequently distal from the promoters of estrogen-regulated genes. Active chromatin-enriched "super-enhancer" (SE) regions, mainly observed in *in vitro* culture systems, often control production of key cell type–determining transcription factors. Here, we defined super-enhancers that bind to ERα *in vivo* within hormone-responsive uterine tissue in mice. We found that SEs are already formed prior to estrogen exposure at the onset of puberty. The genes at SEs encoded critical developmental factors, including retinoic acid receptor α (RARA) and homeobox D (HOXD). Using high-throughput chromosome conformation capture (Hi-C) along with DNA sequence analysis, we demonstrate that most SEs are located at a chromatin loop end and that most uterine genes in loop ends associated with these SEs are regulated by estrogen. Although the SEs were formed before puberty, SE-associated genes acquired optimal ERα-dependent expression after reproductive maturity, indicating that pubertal processes that occur after SE assembly and ERα binding are needed for gene responses. Genes associated with these SEs affected key estrogen-mediated uterine functions, including transforming growth factor β (TGFβ) and LIF interleukin-6 family cytokine (LIF) signaling pathways. To the best of our knowledge, this is the first identification of SE interactions that underlie hormonal regulation of genes in uterine tissue and optimal development of estrogen responses in this tissue.

Estrogen hormones are intricately involved in key molecular events that underlie development of female reproductive tract tissues, optimizing responses to ovarian hormones essential for successful reproduction later in life (1). Many studies of estrogen response mechanisms have utilized *in vitro* cell culture models, which have advanced understanding but are limited in their application to more biological contexts. *In vivo* models of hormone response include the rodent female reproductive tract, which is highly hormone-responsive, facilitating study of mechanisms of tissue development and hormone response. For example, female reproductive tissues of estrogen receptor α (ERα)-null and estrogen-deficient *Cyp19* (aromatase) KO mouse models, both of which resemble their WT littermates at

birth, lack pubertal uterine development, and thus exhibit a hypoplastic uterine phenotype (1–4). These experimental characteristics duplicate those found clinically in patients with insensitivity syndromes due to mutations in their *ESR1* or *CYP19* genes (5–8). Estrogen's activity involves interaction with its nuclear receptor, ERα, which localizes to enhancer regions of chromatin, driven by high affinity for estrogen response element (ERE) DNA motifs. Enhancer regions that ERα interacts with are often distal from promoters of estrogen-regulated genes (1, 9), and current models incorporate a mechanism of chromatin looping to facilitate contacts between enhancer and promoter regions (10, 11). Earlier studies have noted that some enhancers have particularly high enrichment of indicators of active chromatin; these are classified as "super-enhancers" (12, 13). Frequently, these super-enhancers control production of key transcription factors that characterize a particular cell type (12–14). In mice, prior to production of ovarian hormones, which begins with the onset of estrus cyclicity at puberty (postnatal day 28), the prepubertal uterus is hypoplastic, has ERα in all cells, and exhibits rapid transcriptional and growth responses of all uterine cell types to exogenous estradiol (E2) (15–17). The response, however, differs from what is observed in an ovariectomized adult mouse uterus, where the uterus response is restricted to only the epithelial cells (15, 17). Through the process of pubertal maturation, the reproductive tract acquires optimal reproductive functionality (3, 15, 16, 18, 19). The molecular details of this important process have not been explored; therefore, we sought to define the estrogen-dependent enhancer landscape of the developing mouse uterus by analyzing uterine chromatin isolated from prepubertal (21-day-old) or from adult (10-week-old) mice that were ovariectomized (ovexed) to remove the source of endogenous E2 and then treated for 1 h with vehicle (V) or with E2 to gain insights into molecular components and responses impacted during development of a hormonally regulated tissue.

Results

Defining uterine super-enhancers that bind ERα

We defined super-enhancers (SEs) that bind ERα-in prepubertal uterine samples from mice treated for 1 h with vehicle (V) or with E2, as well as in uterine samples from ovexed adult mice treated for 1 h with V or E2 as described under "Experimental procedures." Briefly, ERα-binding enhancers were identified using ERα ChIP-Seq data by stitching together regions with

ASBMB

Published in the U.S.A.

J. Biol. Chem. (2020) 295(25) 8387–8400 **8387**

more than one ERα peak within 12,500 bp in at least one of the samples. The 4634 enhancer stretches containing multiple ERα-binding sites were then classified as "typical" or "super" enhancers (TEs or SEs, respectively) by plotting ranked H3K27Ac signal of each; enhancers beyond the slope = 1 elbow of the curve (Fig. 1*A*) were considered SEs. Therefore, locations of ERα ChIP-Seq peaks from all four sample types were either classified as single peaks (Fig. 1*B*) or were within enhancer regions with multiple peaks (Fig. 1*B*). The multipeak enhancer regions were then classified as super-enhancers or typical enhancers (Fig. 1*B*). Several hundred SEs were identified in each sample type (Fig. 1*A*). Comparison of the enhancers called in each sample indicates that many SEs overlap across the sample types (Fig. 1*A* and Fig. 2), and most that are SEs, but not in all samples, are ranked in the top 25% of enhancers (Fig. 1*A*, *red lines* in the *heatmap below* each *curve*). The SEs in the prepubertal V-treated mice are present before the cells have been exposed to ovarian E2 beginning at puberty, whereas the SEs in the ovexed adult samples represent super-enhancers after the uterus has undergone pubertal maturation. For each super-enhancer curve, genes located at the top 10 SEs are listed. We noted that three of the genes at the SEs (*Zmiz1*, *Ncor2*, and *Rara*) were among the 10 highest ranked in all samples (Fig. 1*C*). Comparison of the SEs using heatmaps of ERα and H3K27Ac ChIP-Seq signals centered on each of the 2431 ERα-binding sites that is within a SE in at least one of the four samples (Fig. 2) indicates that the H3K27Ac signal intensities of the adult and the 21-day-old are similar in V- and E2-treated samples, respectively, showing that the SEs seen in prepubertal samples, prior to pubertal uterine development, are largely unchanged by pubertal development. E2 leads to increased ERα binding at each site, as well as increased H3K27Ac signal flanking SE ERα-binding locations. Interestingly, although E2 also increases ERα binding at the 21,894 non-SE ERα-binding sites (TE and single ERα-binding sites), H3K27Ac signal is more static (Fig. 2), with only the highest ranked ERα binding sites exhibiting E2-dependent H3K27Ac signal increase. Some researchers use H3K4Me1 ChIP-Seq signal intensity, also associated with active enhancers, to classify SEs. Using H3K4Me1 signal to classify uterine enhancers revealed that 65– 87% of SEs by H3K4Me1 were also classified as SEs using H3K27Ac (Table S1). Additionally, >98% of SEs by H3K4Me1 signal were within the top quartile of the H3K27Ac signal. Locations of SEs called using H3K27Ac in the adult ovexed 1-h E2 uterus relative to genes and chromosomes are illustrated in Fig. S1.

Chromatin interactions in uterine tissue

Distal enhancers can exert transcriptional control by physically contacting gene promoters through "looping" mechanisms (10). It is not known whether contacts are dynamically formed in order to exert regulatory signals between distal enhancers and promoters, whether loops are preformed and the activity of the promoters is mediated via dynamic transcription factor interactions, or whether a combination of mechanisms occurs (20). Assigning ERα-interacting regions to regulated genes is important for understanding how ERα binding to distal enhancers regulates gene promoters; therefore, we analyzed ovariectomized adult mouse uterus 1 h after treatment

with V, E2, or progesterone (P4) using Hi-C. We used the Juicer tool to call loops from the Hi-C data of each treatment as well as differential loops in pairwise comparisons (Fig. 3*A*). We observed little variability between replicates or between different treatments, suggesting that loops are not altered globally by the hormone treatments we administered (Fig. 3*A*). Therefore, we combined the loops from all WT samples into an "atlas" of uterine loops. Then we used cohesin subunit SMC1a ChIP-Seq to assess interactions and potential impacts of hormone treatment. Because cohesin slides along chromatin until it contacts a pair of converging CTCF sites (10, 21), we compared SMC1a peaks at loop anchors selected to have cohesin at both ends as a surrogate for the presence of a loop in the sample. We examined SMC1A signal intensity, both at selected loop anchors and at other locations, and compared V– and E2–treated samples (Fig. 3*B*). When we compared V *versus* E2 SMC1a signal intensity, we did not observe a notable impact of E2 treatment (Fig. 3*B*) at selected loop anchors or at other locations, suggesting once again that loops are preformed and not impacted by our hormone treatments. To assess whether specific transcription factors might be associated with V *versus* E2 loops, we analyzed the DNA motifs associated with SMC1a peaks that were located at both ends of loops. The CTCF motif is highly enriched in SMC1a peaks at loop anchors of both V and E2 samples (Table 1). The ERα motif estrogen response element and ERα "tethering" factor motif SP1 are both selectively enriched at SMC1a peaks of the E2 sample. These observations suggest E2-induced mechanisms in which ERα and associated transcription factors such as SP1 interact with preformed chromatin loops. Consistent with this mechanism, we note that Hi-C analysis of uterine tissue from mice lacking ERα shows that loops are present and do not differ from WT samples any more than the variation observed between replicates (Fig. 3*A*).

Super-enhancers are predominantly located in loop ends and are associated with uterine genes

Next, we evaluated the relationships between SEs and chromatin loops and whether SE and uterine genes are brought into proximity in 3D space. For this part of our analysis, we focused on the adult ovexed E2-treated samples. First, we examined average H3K27Ac signal per loop at all loop ends or "anchors" (Fig. 4*A*), which indicated that this histone modification was centered on the ends of loops. By further comparing loop anchors overlapping TEs *versus* SEs, we observed significantly more H3K27Ac signal at TE-associated loop anchors than at all loop anchors ($p < 0.0001$; Fig. 4*A*). Signal was further enriched at SE-associated loop anchors relative to all or to TE-associated loop anchors ($p < 0.0001$), reflecting the more robust enhancer activity and confirming these regions as SEs. Of the 281 SEs identified in adult E2-treated tissue, 94% (263 SEs) were at the end of a loop, suggesting that they were likely to contact genes in distal regions (Fig. 4*B*). To get an indication of the gene regulation that might occur by looping between genes and SEs, we selected genes that either were at one of the SEs in a loop end or were at the other end of a loop that formed from a SE. Altogether, we found this entailed 1600 genes (Fig. 4*C*). Our previous studies have indicated that ERα interaction with chromatin occurs within 1 h and that resulting gene regulation occurs
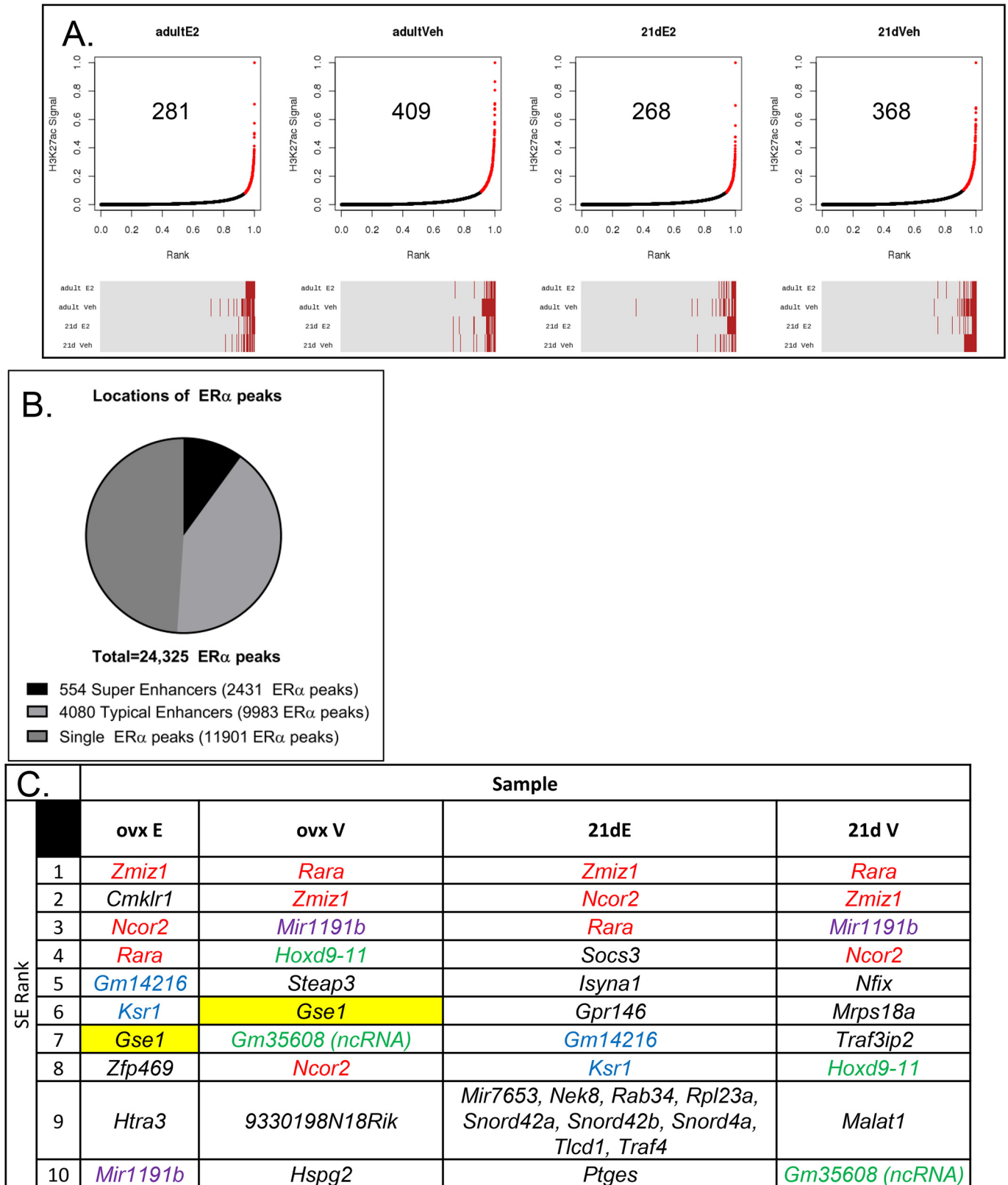
Figure 1. Defining super-enhancers in mouse uterine tissue. *A*, ranked H3K27Ac signal at 4634 regions with >1 ERα-binding site within 12,500-bp regions from uterine samples of 21-day-old or adult ovexed mice treated for 1 h with V or E2 (1 h). The plots show the distribution of the rescaled scores per sample. The *red points beyond* the *elbow* of the *curve*, where slope = 1, are classified as super-enhancers. The enhancer status (typical (*gray*) or super (*red*)) for each peak in each of the four samples in the same order as the corresponding plot *above* it is shown *below* each curve. *B*, proportion of ERα ChIP-Seq peaks that are single peaks or that are in regions with multiple ERα ChIP-Seq peaks within 12.5 kb that were classified as super-enhancers in at least one sample or typical enhancers (not a super-enhancer in any sample) in the above analysis. *C*, genes that are colocalized with the 10 top-ranked SE regions of each sample are listed. The top 10 SEs shared by all four samples are in *red text*, SEs that are in the top 10 in all samples except 21-day E2 are in *purple text*, SEs in the top 10 only in ovexed samples are *highlighted* in *yellow*, SEs that are in the top 10 only in V sample are in *green text*, SEs that are in the top 10 only in E2 samples are in *blue text*.
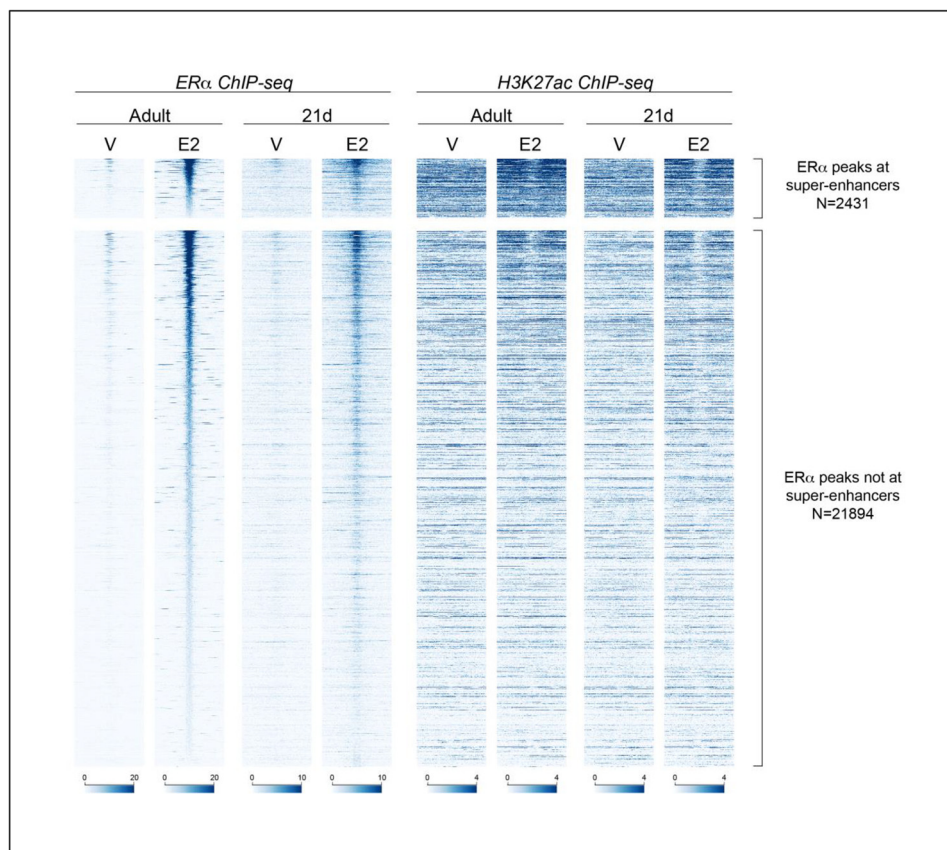
Figure 2. Estrogen increases ERα and H3K27Ac enrichment at super-enhancers. Shown is a heatmap of ERα ChIP-Seq and H3K27Ac ChIP-Seq signal centered on 2431 ERα peaks that are at super-enhancers (*top*) or 21,894 ERα peaks that are not at super-enhancers but are at typical enhancers or are single ERα-binding sites (*bottom*) in uterine chromatin samples from adult ovexed or 21-day-old female mice treated with saline V or with E2 for 1 h. For each set, enhancers are in the order of ERα signal in the adult E2 sample. Each *panel* shows ChIP-Seq signal at ±1 kb relative to the ERα peak midpoint, with signal depth-normalized to 20 million uniquely mapped nonduplicate reads/sample.

subsequently (9, 22). Therefore, we used RNA-Seq of uterine RNA from ovariectomized mice treated with V or treated with E2 for 2 or 6 h to determine whether these 1600 ERα-binding SE-associated genes were transcribed and E2-regulated in the uterus. Indeed, 963 of these 1600 SE-associated genes are expressed (transcripts per million (TPM) $\geq$ 1 in at least one treatment condition) in uterine cells (Fig. 4C). Overall, 9975 uterine genes are regulated by E2 (TPM $\geq$ 1, adjusted p value <0.01) in at least one treatment condition (Table S2). 569 of the 963 uterine SE-associated genes are regulated by estrogen (Fig. 4D and Table S3). This suggests that ERα-binding SEs may be involved in regulation of 5–6% of E2-responsive uterine genes. The remaining E2-regulated uterine genes are likely to be mediated by ERα interactions at TE or at single ERα-binding sites, as we have previously demonstrated that the ERα is required for uterine E2 genomic response (4, 22). To assess how the 569 SE-associated estrogen-regulated uterine genes impact biological functions, we used INGENUITY PATHWAY ANALYSIS. Genes involved with the promotion of gene transcription, cell survival, and genitourinary tract development and suppression of mortality and apoptosis were apparent (Table 2). Notably, upstream regulators with known roles in uterine function, such as estrogen and cytokines, including LIF, a critical mediator of embryo implantation (23), as well as IGF1 and TGFβ (24–32), are identified as activating upstream regulators (Table 3).

Therefore, these ERα-binding SE-associated genes are enriched for important uterine processes.

Super-enhancer–associated genes acquire estrogen responsiveness during postpubertal development

To assess whether postpubertal development impacted E2 regulation of the SE-associated genes identified above, we analyzed gene regulation in 21-day-old and ovexed adult samples from WT mice and mice with deletion of the ERα gene (ERαKO). We treated the mice for 2 h with V or E2 and isolated uterine RNA for microarray. We observed that 245 SE-associated genes were differentially expressed after 2-h treatment with E2. Hierarchical clustering reveals that the responses are ERα-dependent (Fig. S2 and Table S4). What is surprising is that, despite the presence of the SEs prior to pubertal development (Figs. 1 and 2), estrogen regulation is much more robust in adult ovexed samples (Fig. S2 and Table S4), indicating that these genes acquire the transcriptional response as a result of pubertal development.

Super-enhancers are associated with key uterine factors

Our analysis has indicated an association between ERα-mediated responses and looping between SEs and estrogen-regulated genes. Because genes at the SE often encode factors critical for specific cell types (14), we evaluated examples of four
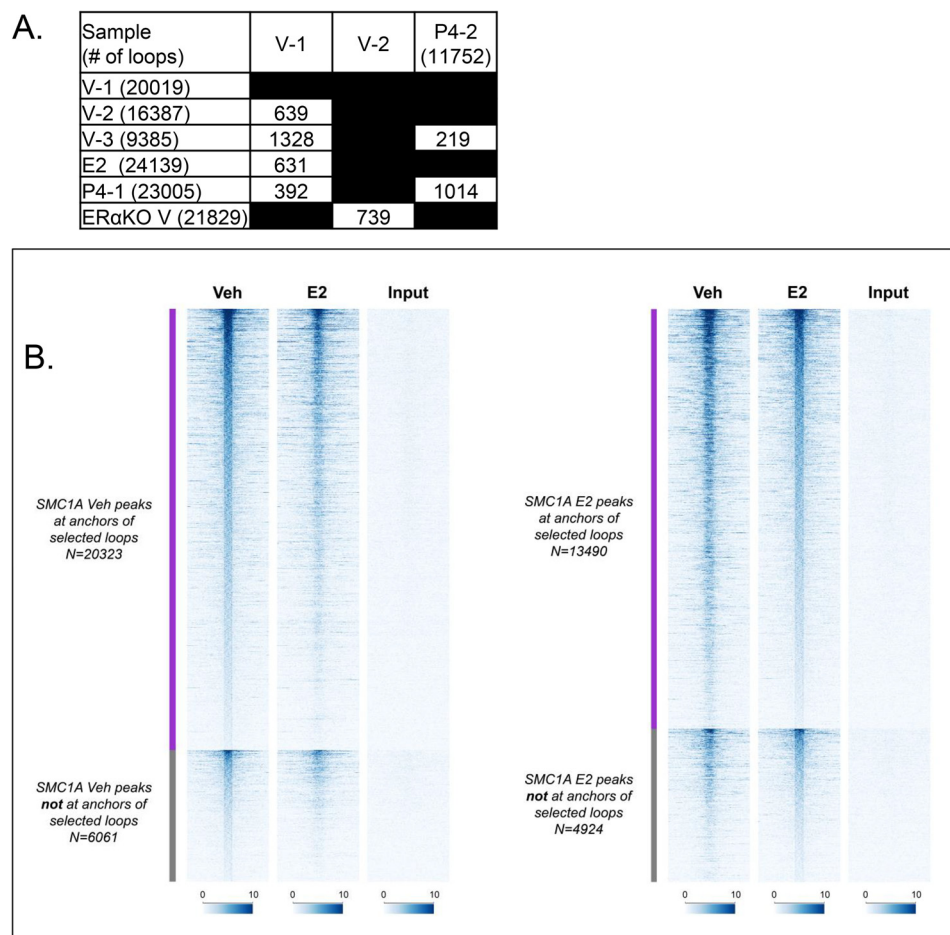
A.

Sample (# of loops)	V-1	V-2	P4-2 (11752)
V-1 (20019)			
V-2 (16387)	639		
V-3 (9385)	1328		219
E2 (24139)	631		
P4-1 (23005)	392		1014
ERαKO V (21829)		739	

B.

Figure 3. E2/ERα does not alter uterine loops. *A,* Juicer output showing the number of loops called from each sample in parentheses and differential loops called between the indicated pairs. Minimal differences are seen between replicates (V-1, V-2, V-3; P4-1, P4–2) as well as between V and hormone treatment (E2 or P4) or between mice lacking ERα (ERαKO) and WT litter mates (V-2). *B,* an "atlas" of uterine loops was built from the six combined WT sample Hi-C data sets. This collapsed set of loops was then filtered to retain only those with SMC1a ChIP-Seq peaks at both loop ends using either V- or E2-treated SMC1a ChIP-Seq data. The heatmap shows SMC1a signal centered on V (*left*) or E2 (*right*) SMC1a peaks that are (*top*) or are not (*bottom*) at loop ends of the selected loops. Each panel shows ChIP-Seq signal at ±1 kb relative to the SMC1a peak midpoint, with signal depth-normalized to 20 million uniquely mapped nonduplicate reads/sample

genes at the SE that are potentially important for uterine development and E2 transcriptional response and that are among the top-ranked SEs (Fig. 1*A*). Retinoic acid receptor a (*Rara*) is a ligand-dependent transcription factor in the nuclear receptor superfamily (33). Homeobox (Hox) transcription factors are key mediators of anterior-to-posterior developmental patterning of tissues (34). *Ncor2* (SMRT; nuclear receptor corepressor 2) interacts with and activates histone deacetylases, thereby reducing transcriptional activity (35). Zinc finger MIZ domain-containing protein 1 (*Zmiz1*) is a novel transcription factor. We first used RT-PCR of RNA samples from prepubertal (21-day-old) or adult ovariectomized uteri to examine the impact of pubertal development on expression of these four genes. All genes showed increases in E2 response in adult tissues *versus* prepubertal tissues (Fig. 5*A*).

Hi-C analysis indicates distal chromatin loops with SEs at *Rara* (Fig. 5*Ba*), the *Hoxd* cluster (Fig. S3), *Ncor2* (Fig. S4*A*), and *Zmiz1* (Fig. S4*B*) genes. We wondered whether the expression of genes that either directly coincide with the SEs or are within loops would be impacted by E2. Therefore, we looked at expression and estrogen regulation of genes within loops formed at these four SEs. We used our RNA-Seq data to evaluate the

levels and E2 regulation of these genes (Table 4). We assessed the relative level of expression of each gene by computing the average TPM of nine uterine RNA samples (3 replicates each of uterine RNA from animals treated with V or with E2 for 2 or 6 h). We examined the E2 regulation of each gene based on fold change of E2 2-h RNA *versus* V RNA or E2 6-h RNA *versus* V RNA. The *Rara* SE forms loops that include several genes (Table 4 and Fig. 5*Ba*), but only *Rara* and *Igfbp4* were regulated by E2 (TPM $\geq$ 1, FDR *p* value <0.01; Table 4). The *Hoxd* cluster SE coincides with the coding genes for *Hoxd8*, *-9*, *-10*, and *-11* and contacts two additional SEs (Fig. S3*A*). Some of the genes within loops that include the SE are regulated by E2 (Table 4). There is a loop between the *Hoxd* SE and a third SE nearly 30 megabases away, in the Wilms tumor 1 (*Wt1*) gene (Fig. S3*B*). Thus, the *Hoxd* cluster in the uterus appears to be at the core of a very large 3D chromatin structure of SEs. Two SEs are localized at the *Ncor2* coding sequence (Fig. S4*A*). *Ncor2* is one of the most highly expressed genes in the loops that include the SE within it (Fig. S4*A* and Table 4). The *Zmiz1* SE loops with two distal SEs (Fig. S4*B*). *Zmiz1* and several other genes within the loop are expressed (Fig. S4*B* and Table 4).

Table 1
HOMER analysis showing *de novo* motifs in SMC1a peaks that overlap with anchors of loops with SMC1a at both ends (Fig. 3*B*) in V-treated (top) or E2-treated (bottom) samples
Shown is the average TPM (average of V, E2 2-h, and E2 6-h transcripts per million) of transcription factors that bind to motifs. ∗, ratio of the percentage of target with motif to the percentage of background with motif.

V SMC1A peaks at loop ends	Motif (best match)	RNAseq average TPM	Enrichment target/Bkg∗	P-value
GCCCGCTAGTGG	CTCF	75.4	33.03	1e-6224
TGACCGATTTCA	RORC	23.0	16.00	1E-31
CCTCGCAACTGA	MYB	10.7	14.00	1E-21
AGTCATCGGCGG	ZFX	52.2	12.00	1E-17
GATTTAAATCAG	LIN54	14.6	11.00	1E-18
TAAAGTCTCGCGC	SMAD3	36.5	10.00	1E-10
AAGCTGAACT	VDR	2.5	6.00	1E-22
AGCTTTGACGCT	RXRB	42.0	5.67	1E-16
GCGGTTACCGGG	RUNX2	1.8	5.00	1E-09
TGTCGAACGT	HIF1A	168.3	4.00	1E-09
TTTGTCGGCT	Jaspar PB0032.1	unknown	2.87	1E-24
AAACACATTTCG	FOXJ1	4.0	2.78	1E-23
GTATTGCGTT	CEBPa	18.9	2.31	1E-15
E2 SMC1A peaks at loop ends				
CGAGACTTGCAT	Jaspar SD0002.1	unknown	16.00	1.00E-16
GCCCGCTAGTGG	CTCF	75.4	13.32	1E-3306
GTGCCGAACTGT	HIC1	22.8	13.00	1.00E-13
TGAATTGTCTTT	SOX17	35.1	12.00	1.00E-24
CGTCCCTCCGTC	SP1	97.6	10.00	1.00E-10
ATTTACTGTT	EWS:ERG-fusion(ETS)	13.2	7.67	1.00E-16
TTAGCAGTGG	ZBTB3	5.1	6.00	1.00E-09
GGTCACCCTGAC	ERE	187.5	5.05	1.00E-47
GGGTTTTCTA	REL	6.8	4.50	1.00E-06

To experimentally determine whether a SE ERα-binding site can impact expression of genes within Hi-C defined chromatin loops, we examined expression levels of genes within loops from a previously described SE distal from the *Igf1* gene (36). The *Igf1* SE forms a loop that includes *Tyms-ps*, *Dram1*, *Pmch*, *Parpbp*, *Nup37*, and *Ccdc53* within it (Fig. 5*Bb*). *Pmch* and *Tym-ps* are not expressed (average TPM < 1); *Dram1*, *Igf1*, and *Nup37* are regulated by E2 (Table 4). In our previous study, we disrupted the *Igf1* distal SE by deleting one of its ERα-binding sites (36); using this IGF1enh4KO model, we examined whether the distal SE is important for E2 regulation of genes in the loops that emanate from it. RT-PCR analysis of uterine RNA samples from IGF1enh4KO and WT littermates shows that although E2 regulation of *Igf1* itself was affected by disrupting the SE (Fig. 5*C*), no change in expression of *Dram1*, *Nup37*, or *Parpbp* occurred, indicating that the deleted site selectively impacts only *Igf1* expression.

Mouse uterus super-enhancers differ from those in breast cancer cells

To evaluate how the mouse uterine SEs might be related to SEs in other E2-responsive cells, we compared our findings with a similar analysis that defined SEs that bind ERα in the MCF-7

breast cancer cell line grown in hormone-deprived medium (37). We compared the genes that are closest to 227 MCF-7 SEs with a list of genes closest to 281 uterine tissue SEs (Fig. 6). After removing genes that do not have both mouse and human orthologs (Fig. 6*A*), about 10% of the SE genes were common between the mouse uterus and MFC-7 cell systems (Fig. 6*B*). The small number of SEs located at genes shared in MCF7 cells and uterine tissue is likely due to differences in the biological responses E2 elicits in a normal E2-responsive tissue (mouse uterus) *versus* an immortalized breast cancer–derived cell line.

Discussion

The importance of E2 and ERα in uterine maturation is emphasized by the observation of hypoplastic uterine tissue in adult-aged ERα-null mice (4), which circulate high levels of E2 but have no receptor protein, and in mice lacking *Cyp19*, which are therefore unable to synthesize E2 (2, 38) but have normal levels of ERα. We defined the estrogen-dependent enhancer landscape of the developing mouse uterus and observed that overall, most of the 21-day-old and adult SEs had similar characteristics; in general, both ERα and H3K27Ac signals are increased by E2 at the SE (Fig. 2). Although E2 increases ERα signal of TE and single ERα-binding sites as well, H3K27Ac is less impacted by E2 (Fig. 2), with only the highest-ranked ERα-binding sites showing an increase. Overall, this suggests that the enhancer landscape necessary for uterine maturation is already in place by postnatal day 21. It was clear, however, from our gene regulation analyses, that pubertal development leads to more robust regulation of genes associated with these SEs (Fig. S2).

Comprehensive analysis of ERα interaction with chromatin using ChIP-Seq has revealed that ERα-binding regions are often distal from coding genes, which has led to a need to understand the 3D structure of chromatin within ERα-expressing cells. We noted that all ERα-binding loop ends had significantly more H3K27Ac signal, centered on the loop anchor, than loop anchors in general (Fig. 4*A*), especially those at super-enhancers. This highlights the importance of ERα in the mechanism of activation via these 3D structures. We did note that H3K27Ac signal is greater at loop ends with TE (Fig. 4*A*), indicating a significant role of these ERα-binding regions in E2 response as well. How responses mediated by single ERα-binding sites or by TE *versus* SE impact uterine development and biological processes will be an important focus of future study. Our previous work characterized one such gene mechanism by deleting an ERα-binding site in a super-enhancer distal from the *Igf1* gene, resulting in loss of E2 induction of the coding transcript (36). Deleting one of the five distal ERα-binding sites did not impact E2-dependent ERα binding to the four remaining distal sites or to a site near the promoter; however, E2-dependent recruitment of the histone acetyltransferase p300 and the cohesin subunit SMC1a was decreased at neighboring sites, and E2-dependent induction of enhancer RNA and coding mRNA transcription was lost (36). Thus, E2-dependent recruitment of factors necessary to optimize enhancer-promoter–mediated *Igf1* transcription is governed by a critical site in the distal enhancer. The *Igf1* distal SE also forms chromatin loops that include other genes, some of which are also regulated by
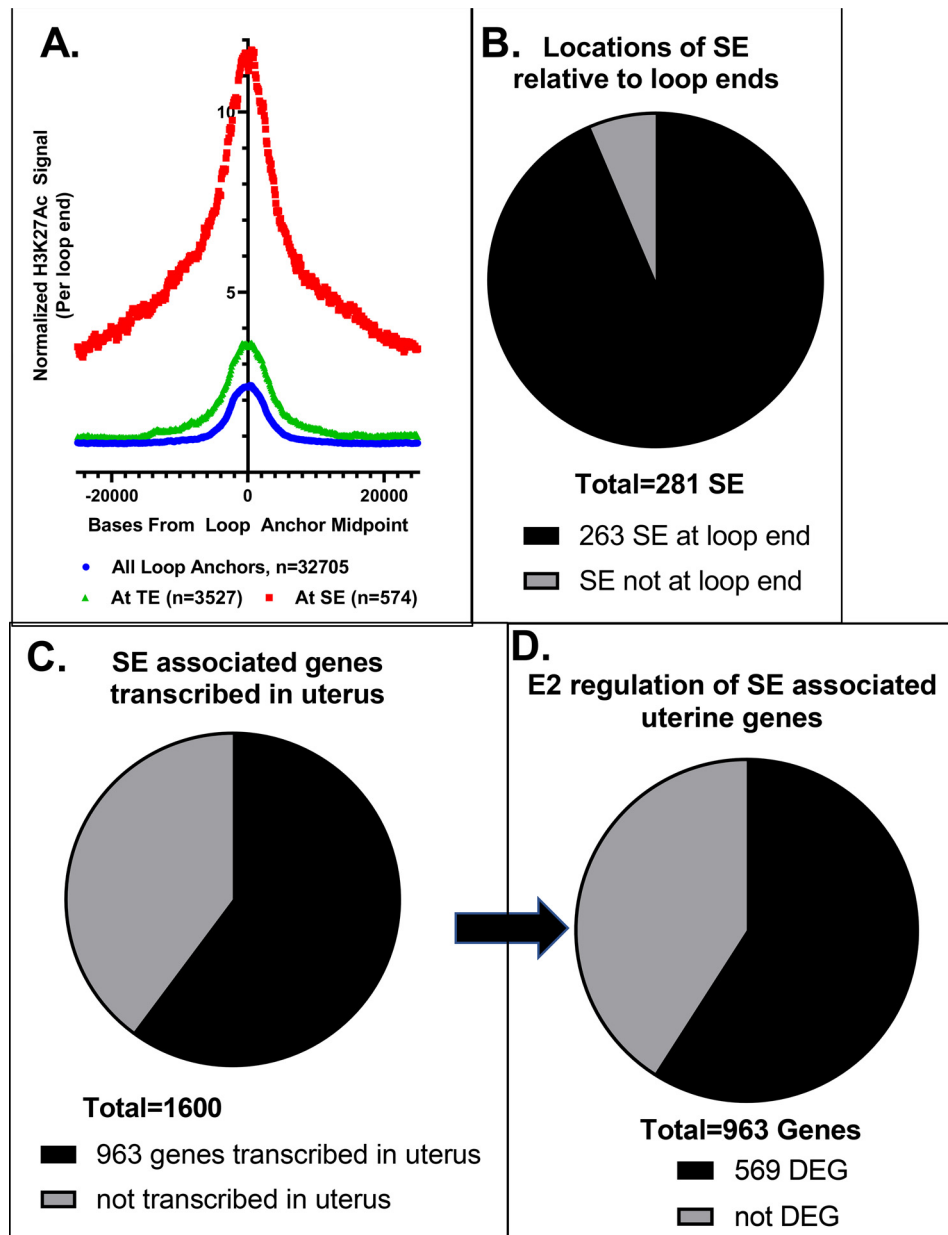
Figure 4. Association of SEs with uterine gene expression. *A*, plot of normalized H3K27Ac signal in 1-h E2 adult ovexed sample per called loop end from the same sample. Curves are from all called loop ends, loop ends at TEs, and loop ends at SEs. *B*, proportion of adult E2 1-h SEs that are in E2 1-h called loop ends. *C*, proportion of 1600 SE-associated genes (at adult E2 1-h SEs that overlap a loop end or at the other end of the SE loop) that are detected in uterine V, E2 2-h, or E2 6-h samples (TPM ≥ 1). *D*, proportion of 963 SE-associated uterine genes differentially expressed (*DEG*; $p < 0.01$) 2 or 6 h after E2 treatment *versus* V treatment.

E2; however, deletion of the ERα-binding site did not change the E2 response of these other genes, indicating that the primary target of the SE in this case is the *Igf1* gene. Whether this relationship between SEs and regulated distal genes is generally seen, or whether there are cases in which expression of multiple genes is impacted by a single SE remains to be studied.

In this study, we identified SEs either in or looping to other well-known highly E2-responsive genes, including *Greb1*, *Lif*, *Fos*, *Cebpb*, *Cyr61*, and *Inhbb* (Table S3). The *Greb1*-interacting super-enhancer identified here was the focus of a previous study indicating the potential role of distal ERα-binding regions in *Greb1* regulation (39). The same ERα-binding region was utilized to model mechanisms of distal interaction in a recent

study (40), highlighting a role for the steroid receptor coactivator, SRC-3, in optimizing contacts between enhancer and promoter regions via interaction with an intronic SRC-3–binding sequence (40). Prior to E2 treatment, the enhancer and promoter are held in proximity to each other through their contacts with SRC-3 bound to the intron. E2 treatment leads to SRC-3–dependent formation of the enhancer-promoter transcriptional complex (40) and, consequently, increased *Greb1* transcription. The formation of structures, such as the SRC-3/intron/enhancer/promoter complex, may be a mechanism utilized by enhancer-promoter interactions.

We note that most of the SEs identified in adult ovexed E2-treated samples were at a loop end (263 of 281; Fig. 4*B*) and

Table 2

Biological functions and diseases associated with 569 E2-regulated uterine genes identified in Fig. 4D

Disease or function annotation	*p*	Activation *z*-score, 2 h	Activation *z*-score, 6 h
Morbidity or mortality	7.47E−08	−5.82	−3.22
Activation of DNA endogenous promoter	9.63E−11	4.30	2.47
Cell movement	3.50E−10	3.99	3.86
Migration of cells	3.89E−08	3.92	3.41
Microtubule dynamics	8.93E−07	3.85	2.41
Development of body trunk	5.71E−10	3.48	2.30
Outgrowth of cells	1.07E−07	3.28	
Cell survival	4.54E−08	3.07	
Organization of cytoskeleton	7.52E−09	3.06	
Organization of cytoplasm	9.02E−09	3.06	
Size of body	2.39E−07	3.06	
Cell movement of endothelial cells	8.57E−07	2.92	2.62
Formation of vessel	4.97E−06	2.73	2.25
Phosphorylation of protein	1.19E−06	2.71	2.25
Apoptosis	1.70E−10	−2.53	−2.28
Development of genitourinary system	1.30E−09	2.51	2.18

Table 3

Upstream regulators enriched in 569 E2-regulated uterine genes identified in Fig. 4D

Upstream regulator	Activation *z*-score, 2 h	Activation *z*-score, 6 h	*p* value of overlap
TGFB1[a]	5.32	5.27	1.77E−11
β-Estradiol	4.63	4.54	1.16E−12
LIF	3.12	2.29	3.01E−05
Cytokine[b]	3.06	3.06	1.3E−06
PGR	2.92	2.92	5.14E−07
Ige	2.62	2.07	2.86E−05
GDF2	2.61	2.61	2.44E−06
ERK1/2[c]	2.50	2.62	2.84E−05
IGF1	2.35	4.41	3.49E−06
α-Catenin	−2.51	−2.11	1.22E−10

[a] Includes TGFB1, TGFB3, and SMAD3.
[b] Includes CSF1, CSF2, EDN1, IFNG, IL1, IL17A, IL1A, IL1B, IL2, Il3, IL4, IL6, OSM, TNF, and TNFSF11.
[c] Includes EGF, ERBB2, MAPK3, MAPK8, MAPK9, and p38 MAPK.

were likely to be at or form a loop to genes expressed in the uterus (Fig. 4C). Many of these SE-associated genes are involved in transcription and in pathways important for uterine function, such as *p53* (41) and *Tgfβ* (26) signaling; therefore, these SEs are associated with important mediators of uterine maturation and function. We did not observe a SE at the *Esr1* gene, although ERα is detected in all uterine cells and SE-associated genes are often characteristic of a particular cell type. Perhaps we should have expected that ERα is not driven by a SE, as we know that the ERα-null mouse develops all uterine cell types normally (4, 42). We did see that *Esr1* was found to be one of the genes closest to an ERα-binding SE in both the MCF-7 cell and our uterus data sets (Fig. 6C). When we examined the impact of E2 on expression of the 963 SE-associated uterine genes, 569 were regulated by E2, a small portion of the 9975 uterine genes that are regulated by E2 (Fig. 4D and Tables S2 and S3). These SE-associated differentially expressed genes (DEG) are involved with activation of TGFβ and estrogen responses and with cytokine pathways, including LIF, a cytokine that is critical for embryo implantation (23) (Table 3).

Our finding of a SE overlapping the uterine *Rara* gene confirms the association of SE with key genes that determine cell fate (12, 13), as critical roles for retinoic acid (RA) signaling in uterine development have been described. RARα is activated by retinol derivatives (Vitamin A), and disruption of retinol signal-

ing, either by disrupting the *Rara* gene or with a retinol-deficient diet, impacts female reproductive tract development (43, 44). RA is required for Mullerian duct development and for maintenance of epithelia of adult female reproductive tracts (45). Mechanistically, retinoic acid signaling influences uterine *versus* vaginal epithelial differentiation (46); therefore, precise regulation of RA signaling mediators is important for normal development and function. This is partly achieved via regulation of enzymes involved in retinoic acid synthesis and degradation (47), but clearly RAR expression is needed to mediate the signal, suggesting that SE in the *Rara* gene plays an important role in female reproductive tract development and function. Additionally, inappropriate perinatal estrogen exposures are known to disrupt the normal patterning of female reproductive tract mesenchyme, but this effect can be prevented by co-treatment with RA (45), illustrating an interplay between estrogen and RA signaling during female reproductive tract development. Evaluation of the *Rara* SE showed that it is within chromatin loops that include two members of the DNA replication complex, *Cdc6* and *Top2a* (Fig. 5Ba and Table 4), which may indicate a role for the *Rara* SE in expression of genes involved in growth responses to E2.

There are four Hox clusters in the mouse genome (*Hoxa*, *Hoxb*, *Hoxc*, and *Hoxd*), and *Hox9–13* are believed to have arisen from a single ancestral gene (48). The *Hoxa* cluster, in particular, has been shown to play a key role in reproductive tract development and function (34). We were interested, then, to note that one of the top ranked prepubertal V SEs was located in the *Hoxd* cluster. *Hoxa* factors are expressed in a progressive pattern in the developing female reproductive tract, with *Hoxa9* in the oviduct, *Hoxa10* in the uterus, and *Hoxa11* in the cervix (34). *Hoxd9*, *-10*, and *-11* are expressed similarly to their *Hoxa* counterparts in the female reproductive tract (49) (Fig. S5A). A role for *Hoxd* in uterine function has been described using complementation studies with *Hoxa*- and *Hoxd*-deleted mice (49). In addition, a recent study evaluated the impact of deletion of one allele each of *Hoxa9,10,11*, *Hoxc9,10,11*, and *Hoxd9,10,11* on uterine development. This study indicated that the combined deletion of one allele each of these nine *Hox* genes greatly decreased uterine gland development (50), further showing a role for *Hoxd* genes in uterine function. Although the *Hoxa* cluster has been very thoroughly described and characterized for its role in uterine function, we did not find any SEs at this gene cluster (Fig. S5B). We do observe chromatin loops between the *Hoxa* cluster and a region more than 1 megabase from the *Hoxa* cluster that includes SEs (Fig. S5B).

Ncor2, also called SMRT (silencing mediator of retinoic acid and thyroid hormone receptor), was originally described as a corepressor for RAR and TR, mainly through its interactions with these receptors and its associated histone deacetylase activity (35). Further study has revealed its dual role as a gene-selective co-activator and co-repressor for ERα (51, 52). A role for NCOR2 in the uterus has not been investigated, but considering its potential to regulate responses of TR, RAR, and ERα, it is noteworthy that we see two SEs in the *Ncor2* gene (Fig. S4A). Recently, it was shown that removing *Ncor2* disrupts formation of a retinoid gradient in mouse embryos and leads to perturbation of HOXC expression patterns, greatly impacting proper
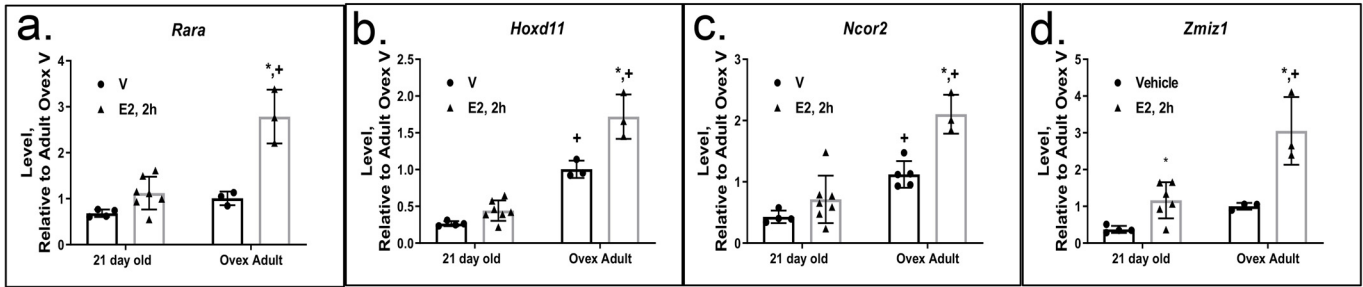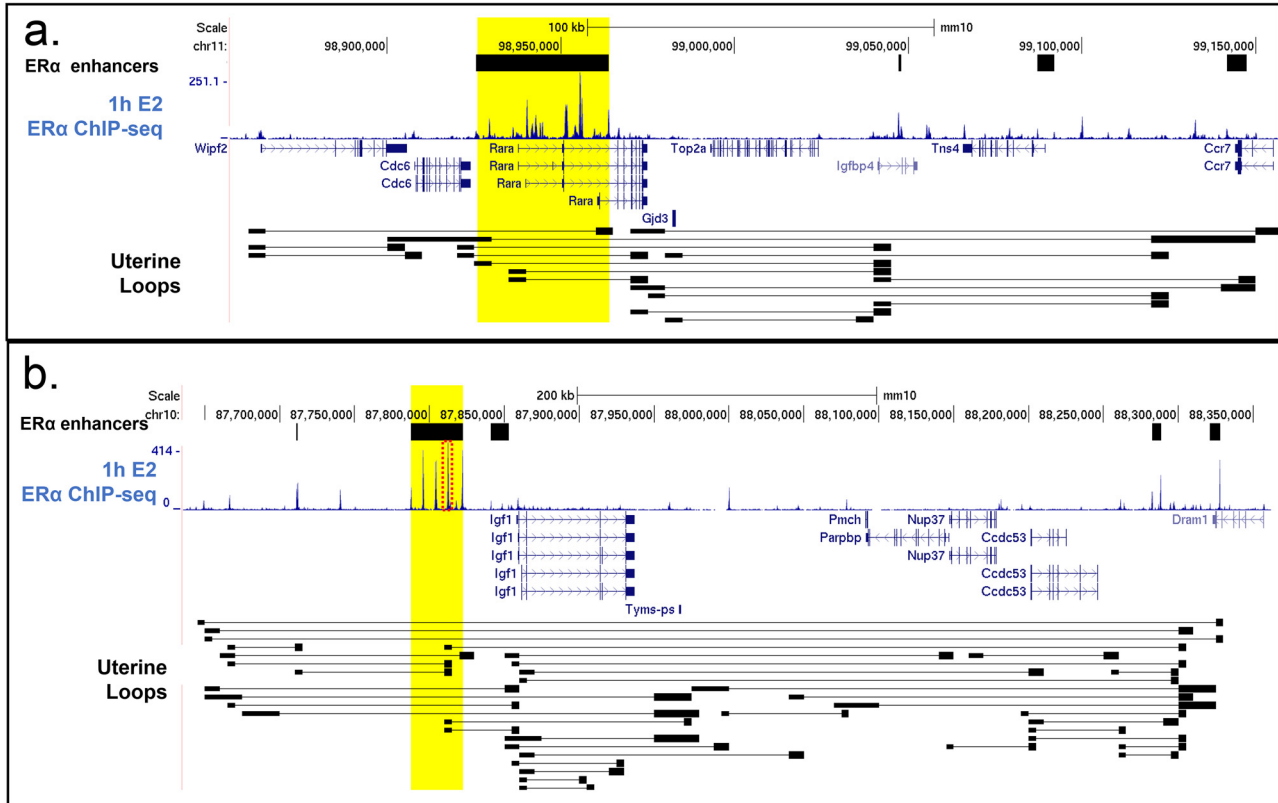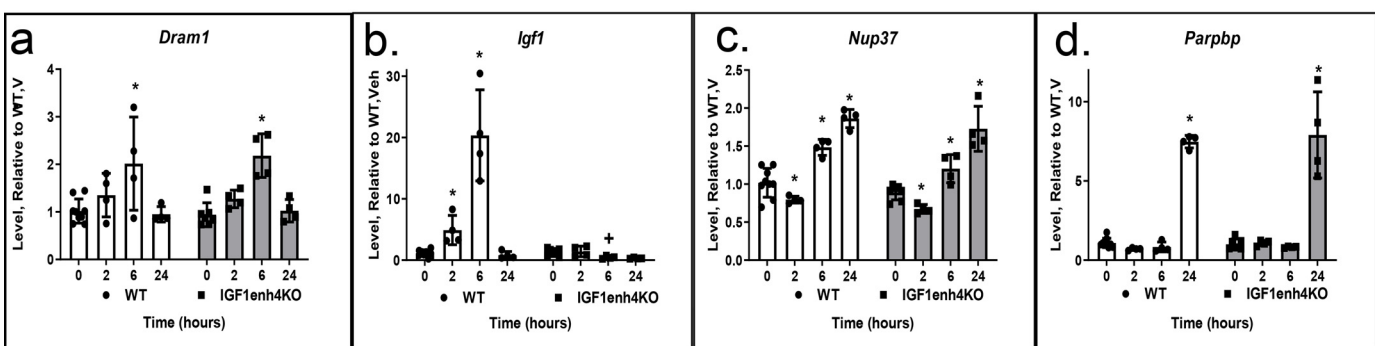
Figure 5. Uterine factors at SEs. *A*, RT-PCR of uterine RNA isolated from 21-day-old or ovexed adult mice treated for 2 h with V or with E2. *a, Rara; b, Hoxd11; c, Ncor2; d, Zmiz1*; *, $p < 0.05$ *versus* V; +, $p < 0.01$ *versus* 21-day-old. *B*, chromatin loops between genes at SE and distal transcripts. SE are indicated by *black blocks*. Chromatin loops from uterine Hi-C samples are indicated by *thin black lines*. Shown are UCSC Genome Browser screenshots of the following. *a, Rara* (Chr11;mm10; chr11:98,854,783–99,160,103) near the SE (*yellow highlight*) at the *Rara* transcript. *b, Igf1* (Chr10; mm10 chr10:87,635,437– 88,361,810) near the SE (*yellow highlight*) distal from *Igf1*. The ERα-binding site that was deleted in IGF1enh4KO is *outlined* in *red*. *C*, disrupting the ERα-binding site in SE distal from *Igf1* prevents E2 induction of *Igf1* but does not alter expression of other genes that contact the SE or that are within the loop. Shown is RT-PCR of RNA from ovariectomized IGF1enh4KO or WT littermates that were treated with V (0) or with E2 for 2, 6, or 24 h. *a, Dram1; b, Igf1; c, Nup37; d, Parpbp.* *, $p < 0.05$ *versus* V; +, $p < 0.05$ *versus* WT.

Table 4
RNA-Seq values for genes within loops of each SE
SE genes are highlighted in yellow. Boldface type shows FDR <0.01 *versus* V.

| Gene Symbol	average TPM	fold change: E2, 2h vs. V	fold change: E2, 6h vs. V
Rara			
Cdc6	5.0	1.36	1.84
Gjd3	0.1	1.32	1.11
Igfbp4	328.6	-1.08	**-1.49**
Rara	28.3	**1.85**	**2.11**
Tns4	10.2	-1.24	1.96
Top2a	69.3	1.42	1.46
Wipf2	8.9	1.07	1.02
Hoxd cluster			
Atf2	43.4	1.06	-1.01
Atp5g3	256.7	1.18	**2.22**
Chn1	6.0	-1.06	**2.49**
Chn1os3	0.7	-1.09	-1.39
Cir1	35.3	-1.16	**-3.53**
Gpr155	9.2	-1.24	**-2.62**
Haglr	0.2	-1.88	-2.75
Hoxd3	0.1	-1.29	**-2.05**
Hoxd3os1	7.3	-1.48	**-2.37**
Hoxd1	35.3	1.26	-1.1
Hoxd4	39.5	-1.43	**-2.95**
Hoxd8	71.7	-1.02	1.37
Hoxd9	45.5	-1.15	**-1.48**
Hoxd10	73.0	-1.22	**-1.65**
Hoxd11	23.8	-1.05	-1.23
Hoxd12	0.0	-1.04	1
Hoxd13	0.0	1.2	-1.08
Lnp	17.4	1.03	1.07
LOC102634401	0.2	-1.92	-2.49
Mtx2	79.7	1.09	**1.54**
Ola1	50.9	1.08	**3.14**
Wipf1	14.2	-1.06	-1.15
Ncor2			
Fam101a	0.9	2.11	1.01
Scarb1	25.1	1.06	**-1.65**
Ncor2	29.2	1.47	-1.08
Zmiz1			
4930572O13Rik	0.5	-1.19	-2.71
4931406H21Rik	24.7	2.64	-1.02
Mir3075	25.9	2.02	1.09
Polr3a	35.0	1.05	**1.51**
Rps24	2395.9	1.04	-1.08
Zmiz1	55.8	2.31	1.45
Igf1			
Ccdc53	34.0	-1.05	-1.17
Dram1	29.3	1.11	**2.14**
Igf1	182.5	1.6	**10.84**
Nup37	27.3	1.04	**1.49**
Parpbp	2.3	-1.11	-1.02
Pmch	0.1	-1.19	-1.38
Tyms-ps	0.2	-1.41	2.74
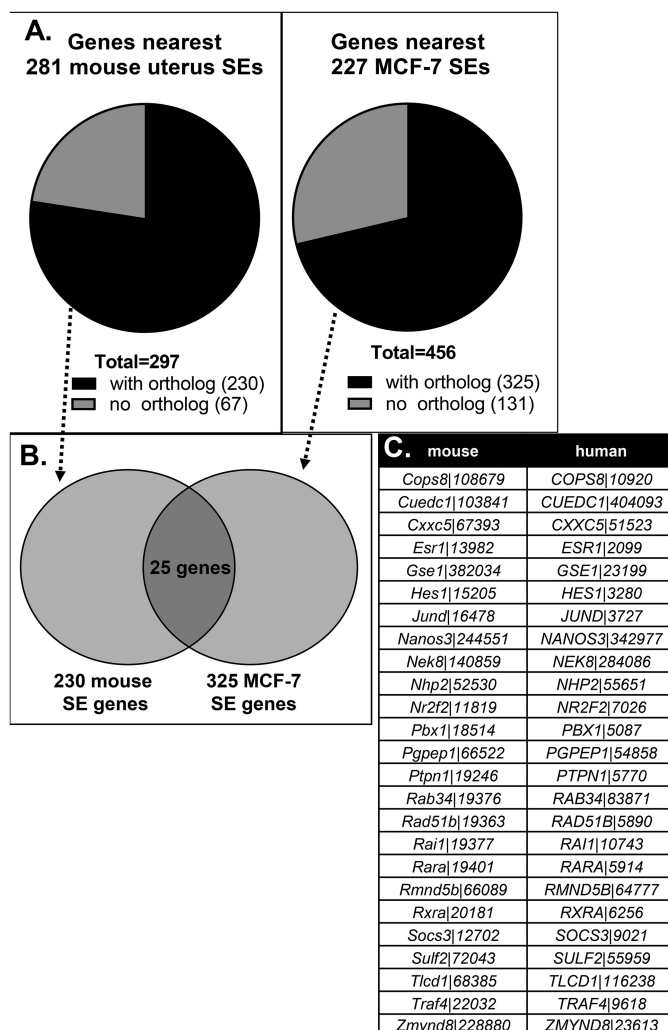
Figure 6. Genes closest to SEs in the uterus differ from those in MCF-7 breast cancer cells. *A*, genes closest to 281 mouse uterus or 227 MCF-7 cell (human) SEs were evaluated for whether they had an ortholog in the other species. Only genes with both mouse and human orthologs were used in the subsequent comparison. *B*, 25 of the genes closest to mouse uterus or MCF-7 cell SEs were shared and are listed in *C*. *C*, *table* listing the gene symbols and Entrez gene IDs of the 25 shared genes from the analysis in *B*.

development (53). The disruptions observed incorporate developmental pathways involving three SE-associated uterine genes (*Ncor2*, *Rara*, and *Hoxd*), suggesting that these SEs might underlie processes important for pubertal development of uterine cells.

Zmiz1 is a member of the PIAS (protein inhibitor of activated STAT) family and was originally identified due to its role in prostate cancer cells as a co-activator that facilitates androgen receptor sumoylation (54). ZMIZ1 regulates activities of certain transcription factors, several of which are important for uterine development and function, including p53 (41), Notch (55), SMAD (24), STAT (56), and androgen receptor (57). Its essential role is highlighted by the finding that its deletion in mice causes embryonic lethality (12). Embryonic fibroblasts isolated from *Zmiz1* null mouse embryos fail to proliferate normally (58, 59), emphasizing its critical cellular role. A missense mutation in *ZMIZ1* has been identified from endometroid cancer samples (Catalogue of Somatic Mutations in Cancer; RRID:

SCR_002260 (60)), and additionally, decreased *ZMIZ1* expression (61) has been reported in adenomyosis biopsies, indicating an essential role for ZMIZ1 in human uterine health as well. We could readily detect *Zmiz1* in the mouse uterus (Fig. 5*A* and Table 4). Its expression was recently noted in rat uterine stromal cells, with down-regulation observed in response to circadian synchronization using the glucocorticoid agonist dexamethasone (62). SE-dependent expression of *Zmiz1* could ensure optimal uterine responses mediated by pathways it regulates; however, the embryonic lethality of the global deletion prevents evaluation of uterine function with current models. We plan to examine its role in uterine tissue via conditional deletion of its expression.

Our approach of identifying super-enhancers in developing uterine tissue is validated by observations that some SEs are at genes encoding factors known to be critical for uterine development and function, such as RARα. The location of most super-enhancers at the ends of chromatin loops and the uterine expression and developmental acquisition of E2 regulation of genes either at SEs or connected by looping to a SE indicate an important role for these enhancers. Indeed, regulatory pathways known to be involved in uterine development and function are impacted by these SE-associated E2-responsive genes. These important regulatory regions likely serve to optimize appropriate, efficient, and timely responses to circulating E2 during each estrous cycle and in preparation for establishing pregnancy.

Experimental procedures

Animals

All mice were used in accordance with an NIEHS-approved animal study protocol and using the 2015 edition of the Public Health Service (PHS) Policy on Humane Care and Use of Laboratory Animals. For E2 response experiments, intact 21-day-old or ovexed adult (10+-week-old) female C57bl6/J mice were purchased from Charles River Laboratories (Raleigh, NC). ERαKO mice (4) (also called Ex3αERKO) and their WT and heterozygous (ERα +/−) littermates were produced in our contract colony at Taconic Farms (Albany, NY). IGF1enh4 KO mice and their WT littermates were produced in our colony at NIEHS and ovariectomized at 10 weeks of age. Genotypes were determined from an ear biopsy by Transnetyx (Cordova, TN). 21-Day-old females were used the week they were received; ovariectomized females were housed for 10–14 days before the experiments to allow endogenous ovarian hormones to diminish. There was no blinding, and mice were randomly assigned to treatment groups. Mice were given a single intraperitoneal injection of 250 ng of E2 (Research Plus Inc., Barnegat, NJ) dissolved in 0.1 ml of normal saline, which is a 10 μg/kg dose. Some were injected subcutaneously with 1 mg of P4 (Sigma) dissolved in 100 μl of sesame oil (Sigma). Control V animals were injected with 0.1 ml of normal saline. Uterine tissue was collected 1, 2, 6, or 24 h after the injections and was snap-frozen in liquid nitrogen. RNA was isolated and cDNA was synthesized for real-time RT-PCR as described previously (22, 36). Primer sequences are listed in Table S5. For gene expression studies, at least three animals per group were used based on an

at least 2-fold change, with a coefficient of variation of 0.2 and 90% power, tested by two-way analysis of variance.

Identification of super-enhancers

Super-enhancers were identified based on the method described by Bojcsuk *et al.* (63). First, 1-h V and 1-h E2 ERα peak calls with high stringency were called by HOMER (parameters: -fdr 0.00001 -F 12 -style factor) for the ovexed adult and 21-day-old samples and then combined via BEDtools mergeBed (version 2.24.0), entailing more than 24,000 ERα-binding locations altogether. BEDtools mergeBed (version 2.24.0) was then rerun, this time to merge all peak calls within 12.5 kb. This set was subsequently filtered to retain only those regions with more than one contributing called peak, resulting in 4634 ERα-binding enhancer regions, each with multiple ERα-binding locations. Each enhancer region was scored by counting the number of overlapping uniquely mapped nonduplicate reads with BEDtools multiBamCov (version 2.24.0); reads in this calculation were H3K27Ac or H3K4Me1 ChIP-Seq data after extension of mapped read length to 200 nucleotides. After normalizing to 20 million reads, the input-subtracted signal was determined per region. The signal curve was plotted as H3K27Ac or H3K4Me1 signal *versus* region rank and rescaled to span 0–1 on both axes. Definition of each enhancer region containing multiple ERα-binding sites as a "typical enhancer" or "super-enhancer" was determined according to the elbow of the signal curve where slope = 1.

SMC1a ChIP-Seq analysis

Processing of the SMC1a ChIP-Seq data was performed as described previously (36). Peak calls were made by HOMER version 4.10.3 via findPeaks with parameter "-style factor". The *de novo* motif analysis was done with HOMER version 4.10.3 findMotifsGenome.pl with parameter "-size given"; for consistency, query regions (SMC1a peaks at loop ends) were resized to 300 bp centered on the midpoint of the called peaks.

RNA-Seq analysis

Processing of the RNA-Seq data was performed as described previously (28). Read counts per gene were determined by Subread featureCounts version 1.5.0-p1 (64) with parameters "-s2 -Sfr -p" for gene models based on RefSeq transcripts as downloaded from the UCSC Table Browser on February 9, 2015. Differential gene analysis was performed with DESeq2 version 1.15.1 (65). Genes were considered expressed in the uterus if TPM $\geq$ 1 in at least one condition. Genes were considered differentially expressed by applying a FDR cutoff of $\leq$0.01. SE-associated genes that were expressed or differentially expressed (FDR < 0.01) in the uterus were identified using the Partek List Manager Tool to find RefSeq gene symbols common to both sets.

Microarray

Two sets of uterine RNA samples were isolated. The first set was obtained from ovariectomized adult ERαKO females and their WT littermates treated for 2 h with V or E2 as above. The second set was obtained from 21-day-old ERαKO females and their WT littermates (produced by timed matings of heterozy-

gous (ERα +/−) males and females) treated for 2 h with V or E2. RNA was assessed by microarray as described previously (66) and analyzed in Partek using analysis of variance to find DEG and then filtering for signal intensity >100 in at least one sample and then filtering for super-enhancer–associated genes. Data from ovariectomized adults (68) (GSE100131) and data from 21-day-old mice (GSE148006) have been deposited in GEO.

Hi-C and data analysis

The Hi-C analysis was based on samples described previously (36) (V-1, E2, and P4-1 in Fig. 3*A*) together with additional samples. Samples V-2 and ERαKO V were processed by Arima Genomics (San Diego, CA), and libraries were sequenced by the NIEHS Molecular Genomics Core, as described for the previous study (36). Samples V-3 and P4-2 were processed and sequenced by Active Motif, Inc. (Carlsbad, CA) using the Arima Genomics Hi-C kit. The Juicer (version 1.5.6) platform was used for processing the Hi-C samples as described previously (36, 67). The quality control metrics from the Juicer output are shown in Table S6. Chromatin loops were identified with the Juicer hiccup utility, an algorithm for finding chromatin loops, by searching for clusters of contact matrix entries with enriched contact frequency relative to local background at default parameters (67). Simple overlap assessment via BEDtools intersectBed was used to determine localization of super-enhancers and SMC1a peaks at loop ends. The "atlas" of mouse uterine chromatin loops was generated by combining Juicer loop calls from the six individual WT samples, whereby all loops with both ends overlapping were collapsed.

Data availability

Hi-C and microarray data from samples are deposited in GEO under GSE147843 and GSE148006.

References

1. Hewitt, S. C., and Korach, K. S. (2018) Estrogen receptors: new directions in the new millennium. *Endocr. Rev.* **39,** 664–675 CrossRef Medline
2. Fisher, C. R., Graves, K. H., Parlow, A. F., and Simpson, E. R. (1998) Characterization of mice deficient in aromatase (ArKO) because of targeted disruption of the cyp19 gene. *Proc. Natl. Acad. Sci. U.S.A.* **95,** 6965–6970 CrossRef Medline
3. Nanjappa, M. K., Medrano, T. I., March, A. G., and Cooke, P. S. (2015) Neonatal uterine and vaginal cell proliferation and adenogenesis are independent of estrogen receptor 1 (ESR1) in the mouse. *Biol. Reprod.* **92,** 78 CrossRef Medline
4. Hewitt, S. C., Kissling, G. E., Fieselman, K. E., Jayes, F. L., Gerrish, K. E., and Korach, K. S. (2010) Biological and biochemical consequences of global deletion of exon 3 from the ER α gene. *FASEB J.* **24,** 4660–4667 CrossRef Medline
5. Quaynor, S. D., Stradtman, E. W., Jr, Kim, H. G., Shen, Y., Chorich, L. P., Schreihofer, D. A., and Layman, L. C. (2013) Delayed puberty and estrogen resistance in a woman with estrogen receptor α variant. *N. Engl. J. Med.* **369,** 164–171 CrossRef Medline
6. Grumbach, M. M., and Auchus, R. J. (1999) Estrogen: consequences and implications of human mutations in synthesis and action. *J. Clin. Endocrinol. Metab.* **84,** 4677–4694 CrossRef Medline
7. Bernard, V., Kherra, S., Francou, B., Fagart, J., Viengchareun, S., Guéchot, J., Ladjouze, A., Guiochon-Mantel, A., Korach, K. S., Binart, N., Lombès, M., and Christin-Maitre, S. (2017) Familial multiplicity of estrogen insensitivity associated with a loss-of-function ESR1 mutation. *J. Clin. Endocrinol. Metab.* **102,** 93–99 CrossRef Medline
8. Lin, L., Ercan, O., Raza, J., Burren, C. P., Creighton, S. M., Auchus, R. J., Dattani, M. T., and Achermann, J. C. (2007) Variable phenotypes associated with aromatase (CYP19) insufficiency in humans. *J. Clin. Endocrinol. Metab.* **92,** 982–990 CrossRef Medline
9. Hewitt, S. C., Li, L., Grimm, S. A., Chen, Y., Liu, L., Li, Y., Bushel, P. R., Fargo, D., and Korach, K. S. (2012) Research resource: whole-genome estrogen receptor α binding in mouse uterine tissue revealed by ChIP-seq. *Mol. Endocrinol.* **26,** 887–898 CrossRef Medline GEO, GSE56501
10. Rowley, M. J., and Corces, V. G. (2018) Organizational principles of 3D genome architecture. *Nat. Rev.* **19,** 789–800 CrossRef Medline
11. Wang, J., Meng, X., Chen, H., Yuan, C., Li, X., Zhou, Y., and Chen, M. (2016) Exploring the mechanisms of genome-wide long-range interactions: interpreting chromosome organization. *Brief. Funct. Genomics* **15,** 385–395 CrossRef Medline
12. Pott, S., and Lieb, J. D. (2015) What are super-enhancers? *Nat. Genet.* **47,** 8–12 CrossRef Medline
13. Sengupta, S., and George, R. E. (2017) Super-enhancer-driven transcriptional dependencies in cancer. *Trends Cancer* **3,** 269–281 CrossRef Medline
14. Hnisz, D., Abraham, B. J., Lee, T. I., Lau, A., Saint-André, V., Sigova, A. A., Hoke, H. A., and Young, R. A. (2013) Super-enhancers in the control of cell identity and disease. *Cell* **155,** 934–947 CrossRef Medline
15. Binder, A. K., Winuthayanon, W., Hewitt, S. C., Couse, J. F., and Korach, K. S. (2015) Steroid receptors in the uterus and ovary. in *Knobil and Neill's Physiology of Reproduction* (Plant, T. M., and Zeleznik, A. J., eds) pp. 1099–1193, Elsevier, Amsterdam

ASBMB

16. Katzenellenbogen, B. S., and Greger, N. G. (1974) Ontogeny of uterine responsiveness to estrogen during early development in the rat. *Mol. Cell. Endocrinol.* **2,** 31–42 CrossRef Medline

17. Quarmby, V. E., and Korach, K. S. (1984) The influence of 17β-estradiol on patterns of cell division in the uterus. *Endocrinology* **114,** 694–702 CrossRef Medline

18. Kelleher, A. M., DeMayo, F. J., and Spencer, T. E. (2019) Uterine glands: developmental biology and functional roles in pregnancy. *Endocr. Rev.* **40,** 1424–1445 CrossRef Medline

19. Stewart, C. A., Fisher, S. J., Wang, Y., Stewart, M. D., Hewitt, S. C., Rodriguez, K. F., Korach, K. S., and Behringer, R. R. (2011) Uterine gland formation in mice is a continuous process, requiring the ovary after puberty, but not after parturition. *Biol. Reprod.* **85,** 954–964 CrossRef Medline

20. Le Dily, F., and Beato, M. (2018) Signaling by steroid hormones in the 3D nuclear space. *Int. J. Mol. Sci.* **19,** E306 CrossRef Medline

21. Gassler, J., Brandão, H. B., Imakaev, M., Flyamer, I. M., Ladstätter, S., Bickmore, W. A., Peters, J. M., Mirny, L. A., and Tachibana, K. (2017) A mechanism of cohesin-dependent loop extrusion organizes zygotic genome architecture. *EMBO J.* **36,** 3600–3618 CrossRef Medline

22. Hewitt, S. C., Deroo, B. J., Hansen, K., Collins, J., Grissom, S., Afshari, C. A., and Korach, K. S. (2003) Estrogen receptor-dependent genomic responses in the uterus mirror the biphasic physiological response to estrogen. *Mol. Endocrinol.* **17,** 2070–2083 CrossRef Medline

23. Chen, J. R., Cheng, J. G., Shatzer, T., Sewell, L., Hernandez, L., and Stewart, C. L. (2000) Leukemia inhibitory factor can substitute for nidatory estrogen and is essential to inducing a receptive uterus for implantation but is not essential for subsequent embryogenesis. *Endocrinology* **141,** 4365–4372 CrossRef Medline

24. Gao, Y., Duran, S., Lydon, J. P., DeMayo, F. J., Burghardt, R. C., Bayless, K. J., Bartholin, L., and Li, Q. (2015) Constitutive activation of transforming growth factor β receptor 1 in the mouse uterus impairs uterine morphology and function. *Biol. Reprod.* **92,** 34 Medline

25. Li, Q., Kannan, A., Wang, W., Demayo, F. J., Taylor, R. N., Bagchi, M. K., and Bagchi, I. C. (2007) Bone morphogenetic protein 2 functions via a conserved signaling pathway involving Wnt4 to regulate uterine decidualization in the mouse and the human. *J. Biol. Chem.* **282,** 31725–31732 CrossRef Medline

26. Li, Q. (2019) Tumor-suppressive signaling in the uterus. *Proc. Natl. Acad. Sci. U.S.A.* **116,** 3367–3369 CrossRef Medline

27. Monsivais, D., Peng, J., Kang, Y., and Matzuk, M. M. (2019) Activin-like kinase 5 (ALK5) inactivation in the mouse uterus results in metastatic endometrial carcinoma. *Proc. Natl. Acad. Sci. U.S.A.* **116,** 3883–3892 CrossRef Medline

28. Kriseman, M., Monsivais, D., Agno, J., Masand, R. P., Creighton, C. J., and Matzuk, M. M. (2019) Uterine double-conditional inactivation of Smad2 and Smad3 in mice causes endometrial dysregulation, infertility, and uterine cancer. *Proc. Natl. Acad. Sci. U.S.A.* **116,** 3873–3882 CrossRef Medline

29. Monsivais, D., Clementi, C., Peng, J., Titus, M. M., Barrish, J. P., Creighton, C. J., Lydon, J. P., DeMayo, F. J., and Matzuk, M. M. (2016) Uterine ALK3 is essential during the window of implantation. *Proc. Natl. Acad. Sci. U.S.A.* **113,** E387–E395 CrossRef Medline

30. Peng, J., Monsivais, D., You, R., Zhong, H., Pangas, S. A., and Matzuk, M. M. (2015) Uterine activin receptor-like kinase 5 is crucial for blastocyst implantation and placental development. *Proc. Natl. Acad. Sci. U.S.A.* **112,** E5098–E5107 CrossRef Medline

31. Nagashima, T., Li, Q., Clementi, C., Lydon, J. P., DeMayo, F. J., and Matzuk, M. M. (2013) BMPR2 is required for postimplantation uterine function and pregnancy maintenance. *J. Clin. Invest.* **123,** 2539–2550 CrossRef Medline

32. Clementi, C., Tripurani, S. K., Large, M. J., Edson, M. A., Creighton, C. J., Hawkins, S. M., Kovanci, E., Kaartinen, V., Lydon, J. P., Pangas, S. A., DeMayo, F. J., and Matzuk, M. M. (2013) Activin-like kinase 2 functions in peri-implantation uterine signaling in mice and humans. *PLoS Genet.* **9,** e1003863 CrossRef Medline

33. Das, B. C., Thapa, P., Karki, R., Das, S., Mahapatra, S., Liu, T. C., Torregroza, I., Wallace, D. P., Kambhampati, S., Van Veldhuizen, P., Verma, A., Ray, S. K., and Evans, T. (2014) Retinoic acid signaling pathways in development and diseases. *Bioorg. Med. Chem.* **22,** 673–683 CrossRef Medline

34. Du, H., and Taylor, H. S. (2015) The role of Hox genes in female reproductive tract development, adult function, and fertility. *Cold Spring Harbor Perspect. Med.* **6,** a023002 CrossRef Medline

35. Cunliffe, V. T. (2008) Eloquent silence: developmental functions of Class I histone deacetylases. *Curr. Opin. Genet. Dev.* **18,** 404–410 CrossRef Medline

36. Hewitt, S. C., Lierz, S. L., Garcia, M., Hamilton, K. J., Gruzdev, A., Grimm, S. A., Lydon, J. P., Demayo, F. J., and Korach, K. S. (2019) A distal super enhancer mediates estrogen-dependent mouse uterine-specific gene transcription of Igf1 (insulin-like growth factor 1). *J. Biol. Chem.* **294,** 9746–9759 CrossRef Medline GEO, GSE125972

37. Miano, V., Ferrero, G., Rosti, V., Manitta, E., Elhasnaoui, J., Basile, G., and De Bortoli, M. (2018) Luminal lncRNAs regulation by ERα-controlled enhancers in a ligand-independent manner in breast cancer cells. *Int. J. Mol. Sci.* **19,** E593 CrossRef Medline

38. Santen, R. J., and Simpson, E. (2019) History of estrogen: its purification, structure, synthesis, biologic actions, and clinical implications. *Endocrinology* **160,** 605–625 CrossRef Medline

39. Sun, J., Nawaz, Z., and Slingerland, J. M. (2007) Long-range activation of GREB1 by estrogen receptor via three distal consensus estrogen-responsive elements in breast cancer cells. *Mol. Endocrinol.* **21,** 2651–2662 CrossRef Medline

40. Panigrahi, A. K., Foulds, C. E., Lanz, R. B., Hamilton, R. A., Yi, P., Lonard, D. M., Tsai, M. J., Tsai, S. Y., and O'Malley, B. W. (2018) SRC-3 Coactivator governs dynamic estrogen-induced chromatin looping interactions during transcription. *Mol. Cell* **70,** 679–694.e7 CrossRef Medline

41. Hu, W., Feng, Z., Teresky, A. K., and Levine, A. J. (2007) p53 regulates maternal reproduction through LIF. *Nature* **450,** 721–724 CrossRef Medline

42. Lubahn, D. B., Moyer, J. S., Golding, T. S., Couse, J. F., Korach, K. S., and Smithies, O. (1993) Alteration of reproductive function but not prenatal sexual development after insertional disruption of the mouse estrogen receptor gene. *Proc. Natl. Acad. Sci. U.S.A.* **90,** 11162–11166 CrossRef Medline

43. Mark, M., Ghyselinck, N. B., and Chambon, P. (2009) Function of retinoic acid receptors during embryonic development. *Nucl. Recept. Signal.* **7,** e002 CrossRef Medline

44. Wilson, J. G., and Warkany, J. (1948) Malformations in the genito-urinary tract induced by maternal vitamin A deficiency in the rat. *Am. J. Anat.* **83,** 357–407 CrossRef Medline

45. Nakajima, T., Sato, T., Iguchi, T., and Takasugi, N. (2019) Retinoic acid signaling determines the fate of the uterus from the mouse Mullerian duct. *Reprod. Toxicol.* **86,** 56–61 CrossRef Medline

46. Nakajima, T., Iguchi, T., and Sato, T. (2016) Retinoic acid signaling determines the fate of uterine stroma in the mouse Mullerian duct. *Proc. Natl. Acad. Sci. U.S.A.* **113,** 14354–14359 CrossRef Medline

47. Nakajima, T., Yamanaka, R., and Tomooka, Y. (2019) Elongation of Mullerian ducts and connection to urogenital sinus determine the borderline of uterine and vaginal development. *Biochem. Biophys. Rep.* **17,** 44–50 CrossRef Medline

48. McGinnis, W., and Krumlauf, R. (1992) Homeobox genes and axial patterning. *Cell* **68,** 283–302 CrossRef Medline

49. Raines, A. M., Adam, M., Magella, B., Meyer, S. E., Grimes, H. L., Dey, S. K., and Potter, S. S. (2013) Recombineering-based dissection of flanking and paralogous Hox gene functions in mouse reproductive tracts. *Development* **140,** 2942–2952 CrossRef Medline

50. Mucenski, M. L., Mahoney, R., Adam, M., Potter, A. S., and Potter, S. S. (2019) Single cell RNA-seq study of wild type and Hox9,10,11 mutant developing uterus. *Sci. Rep.* **9,** 4557 CrossRef Medline

51. Blackmore, J. K., Karmakar, S., Gu, G., Chaubal, V., Wang, L., Li, W., and Smith, C. L. (2014) The SMRT coregulator enhances growth of estrogen receptor-α-positive breast cancer cells by promotion of cell cycle progression and inhibition of apoptosis. *Endocrinology* **155,** 3251–3261 CrossRef Medline

52. Peterson, T. J., Karmakar, S., Pace, M. C., Gao, T., and Smith, C. L. (2007) The silencing mediator of retinoic acid and thyroid hormone receptor (SMRT) corepressor is required for full estrogen receptor α transcriptional activity. *Mol. Cell. Biol.* **27,** 5933–5948 CrossRef Medline

53. Hong, S. H., Fang, S., Lu, B. C., Nofsinger, R., Kawakami, Y., Castro, G. L., Yin, Y., Lin, C., Yu, R. T., Downes, M., Izpisúa Belmonte, J. C., Shilatifard, A., and Evans, R. M. (2018) Corepressor SMRT is required to maintain Hox transcriptional memory during somitogenesis. *Proc. Natl. Acad. Sci. U.S.A.* **115,** 10381–10386 CrossRef Medline

54. Sharma, M., Li, X., Wang, Y., Zarnegar, M., Huang, C. Y., Palvimo, J. J., Lim, B., and Sun, Z. (2003) hZimp10 is an androgen receptor co-activator and forms a complex with SUMO-1 at replication foci. *EMBO J.* **22,** 6101–6114 CrossRef Medline

55. Afshar, Y., Jeong, J. W., Roqueiro, D., DeMayo, F., Lydon, J., Radtke, F., Radnor, R., Miele, L., and Fazleabas, A. (2012) Notch1 mediates uterine stromal differentiation and is critical for complete decidualization in the mouse. *FASEB J.* **26,** 282–294 CrossRef Medline

56. Pawar, S., Starosvetsky, E., Orvis, G. D., Behringer, R. R., Bagchi, I. C., and Bagchi, M. K. (2013) STAT3 regulates uterine epithelial remodeling and epithelial-stromal crosstalk during implantation. *Mol. Endocrinol.* **27,** 1996–2012 CrossRef Medline

57. Walters, K. A., McTavish, K. J., Seneviratne, M. G., Jimenez, M., McMahon, A. C., Allan, C. M., Salamonsen, L. A., and Handelsman, D. J. (2009) Subfertile female androgen receptor knockout mice exhibit defects in neuroendocrine signaling, intraovarian function, and uterine development but not uterine function. *Endocrinology* **150,** 3274–3282 CrossRef Medline

58. Beliakoff, J., and Sun, Z. (2006) Zimp7 and Zimp10, two novel PIAS-like proteins, function as androgen receptor coregulators. *Nucl. Recept. Signal.* **4,** e017 CrossRef Medline

59. Beliakoff, J., Lee, J., Ueno, H., Aiyer, A., Weissman, I. L., Barsh, G. S., Cardiff, R. D., and Sun, Z. (2008) The PIAS-like protein Zimp10 is essential for embryonic viability and proper vascular development. *Mol. Cell. Biol.* **28,** 282–292 CrossRef Medline

60. Tate, J. G., Bamford, S., Jubb, H. C., Sondka, Z., Beare, D. M., Bindal, N., Boutselakis, H., Cole, C. G., Creatore, C., Dawson, E., Fish, P., Harsha, B., Hathaway, C., Jupe, S. C., Kok, C. Y., *et al.* (2019) COSMIC: the Catalogue Of Somatic Mutations In Cancer. *Nucleic Acids Res.* **47,** D941–D947 CrossRef Medline

61. Herndon, C. N., Aghajanova, L., Balayan, S., Erikson, D., Barragan, F., Goldfien, G., Vo, K. C., Hawkins, S., and Giudice, L. C. (2016) Global transcriptome abnormalities of the eutopic endometrium from women with adenomyosis. *Reprod. Sci.* **23,** 1289–1303 CrossRef Medline

62. Tasaki, H., Zhao, L., Isayama, K., Chen, H., Nobuhiko, Y., Yasufumi, S., Hashimoto, S., and Hattori, M. A. (2013) Profiling of circadian genes expressed in the uterus endometrial stromal cells of pregnant rats as revealed by DNA microarray coupled with RNA interference. *Front. Endocrinol.* **4,** 82 CrossRef Medline

63. Bojcsuk, D., Nagy, G., and Balint, B. L. (2017) Inducible super-enhancers are organized based on canonical signal-specific transcription factor binding elements. *Nucleic Acids Res.* **45,** 3693–3706 CrossRef Medline

64. Liao, Y., Smyth, G. K., and Shi, W. (2014) featureCounts: an efficient general purpose program for assigning sequence reads to genomic features. *Bioinformatics* **30,** 923–930 CrossRef Medline

65. Love, M. I., Huber, W., and Anders, S. (2014) Moderated estimation of fold change and dispersion for RNA-seq data with DESeq2. *Genome Biol.* **15,** 550 CrossRef Medline

66. Hewitt, S. C., Li, R., Adams, N., Winuthayanon, W., Hamilton, K. J., Donoghue, L. J., Lierz, S. L., Garcia, M., Lydon, J. P., DeMayo, F. J., Adelman, K., and Korach, K. S. (2019) Negative elongation factor is essential for endometrial function. *FASEB J.* **33,** 3010–3023 CrossRef Medline

67. Durand, N. C., Shamim, M. S., Machol, I., Rao, S. S., Huntley, M. H., Lander, E. S., and Aiden, E. L. (2016) Juicer provides a one-click system for analyzing loop-resolution Hi-C experiments. *Cell Syst.* **3,** 95–98 CrossRef Medline

68. Hewitt, S. C., Winuthayanon, W., Lierz, S. L., Hamilton, K. J., Donoghue, L. J., Ramsey, J. T., Grimm, S. A., Arao, Y., and Korach, K. S. (2017) Role of ERα in mediating female uterine transcriptional responses to IGF1. *Endocrinology* **158,** 2427–2435 CrossRef Medline GEO, GSE100131

ASBMB